12-2017

# Determination of Safe Ballasts for Anchoring Event Tents by Finite Element Analysis

Sandeep Manoharan
*Clemson University*

# DETERMINATION OF SAFE BALLASTS FOR ANCHORING EVENT TENTS BY FINITE ELEMENT ANALYSIS

---

A Thesis
Presented to
the Graduate School of
Clemson University

---

In Partial Fulfillment
of the Requirements for the Degree
Master of Science
Civil Engineering

---

by
Sandeep Manoharan
December 2017

---

Accepted by:
Dr. Vincent Blouin, Committee Co-chair
Dr. Brandon Ross, Committee Co-chair
Dr. Weichiang Pang

## ABSTRACT

Event tents are large structures made of fabric covers attached to a structural frame and poles. Every year, many temporarily installed tents are subjected to large wind conditions that lead to sliding or lift of the frame due to improper anchoring to the ground. When ballasted, as opposed to anchored using stakes that penetrate the ground, non-certified tents are generally installed without proper analysis of sufficient ballast weights, which results into tent movements and lack of safety. The objective of this thesis is to determine load factors for non-certified tents affected by high wind loads. The load requirements (load factors) are determined for typical frame tents to provide ballasting guidelines to tent installers.

A Design of Experiments (DOE) simulation for calculating the responses of different tent configurations under different loading scenarios is developed and conducted. The parameters included in the analysis that defines the size and shape of the tents include: height, width, roof height, roof slope, bay width and wind orientation. The loading scenarios include wind loads from different directions with different intensities prescribed by code. A parameterized finite element model allows to determine the tension forces applied to the attachments points to prevent lift-off and sliding. These forces are then used to determine the safe weight of the ballasts used by installers based on the type of ballast, such as plastic water barrels, steel drum, and concrete blocks, and the type of ground surface, such as asphalt, smooth and rough concrete, grass, dirt, and gravel. These different sets of conditions for any given ballasting configuration are defined by the known friction coefficient between surfaces.

The developed guidelines are intended to be made available to tent installers who will then have more confidence in the safety of any tent installation.

## DEDICATION

This thesis is dedicated to my family and friends who supported me throughout my research period.

## ACKNOWLEDGMENTS

I wish to express my sincere gratitude to Dr. Vincent Blouin, for guiding me throughout my research phase at Clemson University.

I would also like to extend my gratitude towards the Tent Rental Division of Industrial Fabrics Association International (IFAI) for giving me the opportunity and means to perform this research.

In addition, I would like to thank Dr. Brandon Ross and Dr. Weichiang Pang who rendered their help during the period of my project work.

Apart from them, I would also like to extend my thanks to Derek McMullen and Grant Davidson who helped me in conducting experiments at Ravenel Research Laboratory, Clemson University.

## TABLE OF CONTENTS

Page

Table of Contents (Continued)

Page

## LIST OF TABLES

List of Tables (Continued)

Table Page

## LIST OF FIGURES

List of Figures (Continued)

Figure Page

# CHAPTER ONE

# INTRODUCTION

## 1.1 Background and Problem Statement

Tents offer shelter to people on a temporary basis, protection from winds and rain during receptions, ceremonies, and other recreational and professional events. As shown in Figure 1, tents consist of sheets of fabric attached to frames and held to the ground by stakes or ballast weights [1]. These stakes and ballasts are generally connected to the tent by means of ropes called lines guys.

The industry uses two types of tents: (1) engineered and certified tents, which are generally large tents designed and extensively studied by engineering firms that specify requirements for installation and utilization, and (2) non-certified tents, which are generally smaller and only come with installation and utilization guidelines offered by the manufacturer.

The research presented in this thesis is part of a larger research project sponsored by Industrial Fabrics Association International (IFAI) [2]. IFAI is an organization that promotes the use of specialty fabrics, including the design and manufacturing of event tents. The larger project consists of first determining the minimum holding power required to anchor frame tents and pole tents, and then calculate the ballast weights necessary to achieve the holding power for any pre-selected ballasting configuration. This thesis is a subset of the larger project as it focuses exclusively on frame tents and directly finds appropriate ballast weights for holding non-certified frame tents to the ground under any wind condition.

**Figure 1: Example of event tents**

More specifically, the main aim of this project is to find the load factors for various tent configurations and operating conditions which are used to determine the required ballast weights. Using on-field experiments to find out what values of ballast weights are to be used to withstand high winds for any region is physically infeasible. Therefore, the goal was to use an effective way to find out the ballast weights for any configuration anticipated on the field. The method developed in this research consists of using simulation software for analyzing the performance of any tent. Matlab, a scientific programming environment [21], was used to define the parametric description of the tents, and Abaqus, a finite element software [22], was used to perform the numerical static analysis.

### 1.2 Literature review

Wind is an important consideration when constructing, installing and utilizing tents. Mohammadi and Heydari [3] discussed their survey of various studies of seismic and wind loads for temporary structures. Their paper gave importance to wind and seismic loads as

much as live and dead loads while designing temporary structures such as scaffolds, shelters, tents, etc. However, it was noted that live and dead loads are generally negligible compared to wind loads in event tents since they are the lightest temporary structures. Bolduc [4] work reiterates why designing for wind loads is a serious matter and in his paper he examines many cases of roof collapses under wind loads, rain loads and snow loads. Gorlin [5] emphasized that engineers from all states have considered the use of ASCE 7-10, the minimum design loads for buildings and other structures prescribed by the American Society of Civil Engineers [23], for designing wind loads on any structure. This article justified the use of ASCE 7-10 in this research for calculating wind loads on tents.

St. Pierre [13] along with his team conducted wind tunnel experiments on a typical two-story house which included conditions such as a house without surrounding houses and another test with a house among similar houses in various subdivision types such as grid and crescent subdivisions. His team measured pressure at 422 locations on the house model and results proved that wind loads get reduced when surrounded by houses of similar size. Stathopoulos [14] reiterated this statement by proving through his results that pressure coefficients are lower than those specified by wind standards and codes of practice. For this experiment, he carried out a wind tunnel study to examine the effects of various tree configurations on wind-induced air infiltration and structural loading of low-rise buildings. Therefore, in this research, assuming that tents are constructed on spread fields with no obstruction to wind around them, considering wind loads for the design of tents to avoid being blown away was an important task.

The use of a trial-and-error procedure to conduct computer simulation experiments can be prohibitively slow. Lu [9] attributed this statement by saying that Finite Element Analysis (FEA) is preferred due to its resilient feature and easily adapted for various materials, shapes, etc. However, he also noted that in FEA modeling, one should be watchful of the end results. McAlpine [6] indicated the importance of validation of the FEA process by comparing results of FEA models to sample calculations by standard analytical techniques. This kind of validation was shown by Mu and Wu [7] as well. They showed that the computed internal stresses and deformations by FEA model comply with laboratory experimental results. Bail [8] has reiterated this statement in his paper where most of the corresponding results from testing are in agreement with those from FEA models.

Wang [15] in his study on mechanical behaviors of a special joint between a rigid suspension cable and a truss girder in a rigid suspension stiffened steel truss bridge proceeded to use a three-dimensional finite element model only after results obtained from the 3D model was as good as the results of the model test. FEA is used in many areas to cut down the development time. Kurowski [16] proclaimed the idea of using a perfect 3D model for FEA analysis is sometimes faced by some limitations as there will be no proper interaction between 3D CAD model and FEA. He wrote that these CAD models are required to have many modifications before meshing with finite elements. The main exercise is not in obtaining the results from the FEA model and comparing with the sample calculations by conducting experiments on real time structures. Most of the study should be done on examining the most intricate details of the structure which will help in coming

up with a FEA model close to the real time working structure. An excellent match between the FEA designed model and the structure will be possible if there is no way to propose error.

Dinh [10] focused on tension fabric structures and showed severe geometrical and material nonlinearities when analyzed which led him to nonlinear finite element analysis of the membrane structure using Abaqus/standard software. This is one of the reasons why we used Abaqus for our FEA model analysis. In addition, He [17] worked on improving the efficiency of the construction and automated design of temporary structures where he did the parametric and automatic modeling of 3D temporary grandstand structures with Abaqus followed by linear and nonlinear buckling analysis of the structure.

Zhao [11] used Matlab to teach finite element analysis of statically determinate truss structures in his class lecture for various reasons. Few of the main reasons include flexibility in finding forces in truss members along with reaction forces at the fixed and sliding joints. Zhao found his inspiration in Pike [12] who taught FEA for a class through the use software. In his first few lectures he taught them to calculate forces and deflections given geometry, constraints, and loads mathematically. Out of his three demonstrations using software to analyze the truss using FEA, the first two cases had analyzed the way they expected it to happen. But during his third demonstration, he proved them it was easy for the software to analyze geometrically simple but analytically complex system. These facts inspired this research for using Matlab and Abaqus for completing the analysis of the tents represented as truss and frame structures.

Design of experiments (DOE) is a systematic method to determine the relationship between factors affecting a process and the output of that process [20]. DOE is generally used in design for the purpose of optimizing a system or a process. In this research, however, it is used to determine the relationship between design parameters of tents and the load factors and ballast weights.

## 1.3 Research Statement

### Research Questions

Two main research questions are defined in this project and stated as follows:

(1) Assuming that the tent configuration is parametrized, can a design of experiments be developed for a large set of parametric values in order to determine the corresponding load factors and ballast weights?

(2) What are the load factors and ballast weights necessary to safely secure tents under any wind conditions according to code?

### Research Method

This project falls in the realm of simulation research. As described in detail in a subsequent chapter, a Matlab script is used to develop the parametric description of any given tent and the corresponding wind loads. It then creates the FEA input file and calls the FEA software, Abaqus, to analyze the performance of the tent and determine the reaction forces applied on the line guys. Finally, the Matlab script converts the reaction forces to ballast weights using the analytical equations of the three modes of failure, i.e., sliding, tilting and lift of any ballast.

## 1.4 Description of the thesis

The first chapter gave an introduction into event tents and the literature related to the analysis of these tents.

The second chapter describes the tents in more details and the design parameters to be considered for the analysis. It also describes the sections of the codes from ASCE 7-10 which prescribes the methods for calculating the wind loads.

The third chapter describes how the finite element model was developed along with the conversion of the surface wind loads prescribed by code to the concentrated forces applied at the nodes of the tent frame. The first half of the third chapter deals with the introduction to FEA and the second half deals with the procedure for obtaining results from the FEA analysis.

The fourth chapter describes the different modes of failure of the tent that are used to determine the ballast weights. It also presents the derivation of the equations for the respective modes of failure.

The fifth chapter discusses the effect of different parameters of tent which can affect the ballast weight values. The different parameters considered are tent length, tent width, roof pitch angle, pre-tension of guys and wind speed.

The sixth chapter describes the experiments conducted on field to determine the load factors of various types of ballasts and surfaces, which affect the final ballast weights.

Finally, the seventh chapter concludes the thesis with different observations essential to the installation of a tent and the selection of appropriate ballast weights. This chapter also describes future work.

# CHAPTER TWO

# DESCRIPTION OF TENTS AND LOADS

## 2.1 Tent, Frame, and Guys

Tents are structures generally installed for a temporary purpose. A tent is composed of a frame and a preformed reinforced fabric shaped to fit the exterior envelope of the frame. The frame includes vertical columns, called uprights, distributed along the circumference of the tent, and the roof structure. As shown in Figure 2, the tent frame and the fabric are held to the ground by cables or guy lines attached to the fabric at the eave and to the ballasts uniformly distributed around the tent. The tent frames are generally made of galvanized steel or aluminum and the guy lines are made up of steel cables, polymeric straps or ropes. The ballast are either plastic barrels or steel drums filled with water or concrete, or concrete blocks.

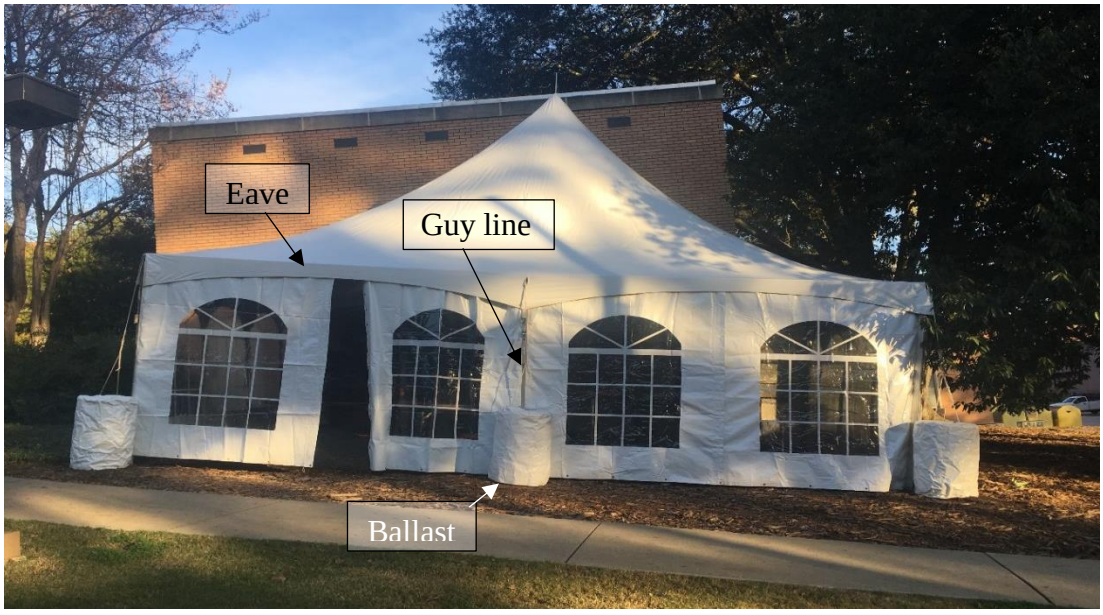


**Figure 2. Illustration of guy lines and ballasts**

The parameters selected in this research for describing the tent are length (L), width (B), pitch angle of the roof (P), number of intermediate posts along the length ($Np_L$), number of intermediate posts along the width ($Np_W$), the angle of the guy lines (alpha), and the pre-tension of the guy lines (PT) (see Figure 3). The different values for all the parameters are listed in Table 1.

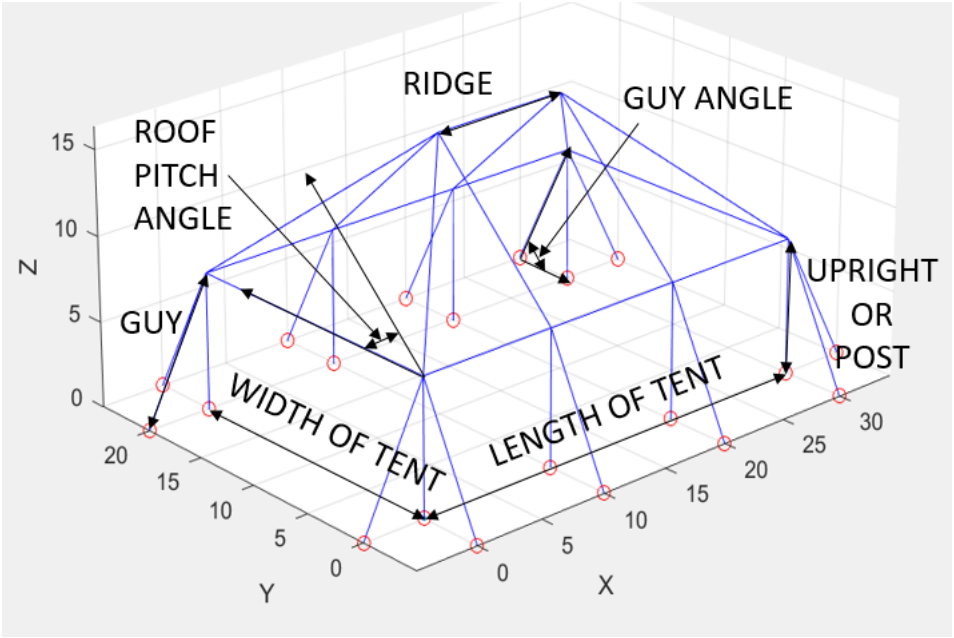


**Figure 3: Diagram showing Length, Width, Roof Pitch Angle, Ridge, Upright or Post, Guy and Guy Angle**

**Table 1: Different parameters considered and their values**

| Parameter | Symbol | Values |
|---|---|---|
| Length | L | 20 ft, 30 ft, 40 ft |
| Width | B | 10 ft, 20 ft, 30 ft |
| Roof Pitch Angle | P | 6 in 12, 8 in 12, 10 in 12 |
| Intermediate posts along Length | $Np_L$ | 2, 3, 4 |
| Intermediate posts along Width | $Np_W$ | 0, 1 |
| Frame stiffness | F | Defined by cross-section data |
| Angle of guy lines | Alpha | 45, 60, 75 |
| Pre-tension of guy lines | PT | 300 lbf to 1500 lbf (100 lbf increments) |

The tent frame used can either be a tubular cross-section, C-channel, I-beam or T-beam. In this research, it is assumed that the type of cross-section does not affect the ballast weights and it is assumed to be a tubular cross-section defined by inner and outer diameters. As the dimensions of the tent vary, the size of the frame cross-section may vary accordingly. The frame connections are assumed to be beam connections, i.e., rigid connections with transfer of moments. The stiffness of the fabric is neglected compared to the overall stiffness of the frame. The tent fabric is attached to the frame using Velcro loops around the frame elements, which means that the fabric may not be fully attached along the length of the frame elements. It is assumed, however, that all corners are secured and rigidly connected.

The fabric must be tightened for stability and aesthetic purposes by applying pre-tension in all guy lines. The pre-tension is applied during installation by tightening the guy lines. Pre-tensioning of guys is a long process that is achieved manually by the installer who must go around the tent to tighten each guy until a pre-tension of 100 lbs to 1500 lbs is applied in each guy depending on the size of the tent.

The roof of the tent is generally fully enclosed. The vertical walls, however, may be entirely closed, partially opened, or entirely opened for ventilation and circulation. The tent is considered enclosed, partially enclosed, and open, respectively. In this research, it is assumed that the tents are partially enclosed since the flexibility of the fabric allows significant entry of air at the space between the fabric and the floor. In any case, this assumption is more conservative than the open configuration since it leads to higher wind loads and therefore higher ballast weights.

## 2.2 Loads defined by code, assumptions and load cases

The wind loads are calculated as per ASCE 7-10 [18] included in Appendix A of this thesis. The procedure used for analyzing these non-certified tents was Main Wind-Force Resisting System (MWFRS) method as opposed to Components & Cladding (C&C) method under the assumption that the overall frame stiffness is greater than overall fabric stiffness. Per ASCE 7-10, C&C method is appropriate for elements having a tributary less than 700 square feet; for this reason, it is suggested that future research can include the C&C method for analyzing these non-certified tents. The wind is considered flowing parallel or perpendicular to the ridge of the tent. The wind load parameters are taken from chapters 26 and 27 of ASCE 7-10, which are included in Appendix 1 for completeness. The wind loads are dependent on the following parameters,

- Basic wind speed, V (Section 26.5),
- Wind directionality factor, $K_d$ (Section 26.6),
- Exposure category (Section 26.7),
- Velocity pressure exposure coefficient, Kz (Section 27.3)
- Topographic factor, $K_{zt}$ (Section 26.8),
- Gust-effect factor (Section 26.9),
- Enclosure classification (Section 26.10), and
- Internal pressure coefficient, ($GC_{pi}$) (Section 26-11).

Basic wind speed, V (Section 26.5 of ASCE 7-10) – The wind velocity is taken from the speed maps or the wind speed website where the latitude and longitude of the

desired location can be entered and the wind speed for different risk categories are presented. In this research, 30 to 70 mph were considered with increments of 10 mph.

Wind directionality factor, $K_d$ (Section 26.6 of ASCE 7-10) – This factor is taken from Table 26.6-1 of ASCE 7-10. Since the tent falls under the category Main Wind Force Resisting System (MWFRS), $K_d$ has a value of 0.85.

Exposure category (Section 26.7 of ASCE 7-10) – The tent is analyzed for the worst condition where there are no obstructions, which corresponds to category D.

Velocity pressure exposure coefficient, $K_z$ (Section 27.3 of ASCE 7-10) – Choosing the exposure category D (assuming it is installed on a flat site, unobstructed area around the tent), the $K_z$ value differs according to the height of the tent and is taken from Table 27.3.1 of ASCE 7-10.

Topographic factor, $K_{zt}$ (Section 26.8 of ASCE 7-10) – The value for $K_{zt}$ is taken as 1, since it is assumed that tent is situated on level ground.

Gust-effect factor (Section 26.9 of ASCE 7-10) – The factor for tents is taken as 1 as they are considered as flexible buildings.

Enclosure classification (Section 26.10 of ASCE 7-10) – As mentioned earlier, in this research, it is assumed that the tents are considered partially enclosed.

Internal pressure coefficient, ($GC_{pi}$) (Section 26-11 of ASCE 7-10) – As tents are considered partially enclosed, $GC_{pi}$ is defined as +/- 0.55. This means that two cases are considered: +0.55 for outward internal pressure and -0.55 for inward internal pressure.

The velocity pressure, $q_z$, evaluated at height z measured from the ground is calculated by the following equation:

$$q_z = (0.00256).K_z.K_{zt}.K_d.V^2 \ (lb/ft^2) \quad (1)$$

$$p = q.G.C_p - q_i.(GC_{pi}) \ (lb/ft^2) \quad (2)$$

where

$q = q_z$, corresponds to windward walls evaluated at height z above the ground,

$q = q_h$ corresponds to leeward walls, side walls, and roofs, evaluated at the roof mean height h,

$q_i = q_h$ corresponds to windward walls, side walls, leeward walls, and roofs for negative internal pressure evaluation in partially enclosed buildings,

G = gust-effect factor is taken from Section 26.9,

$C_p$ = external pressure coefficient considered from Figs. 27.4-1,

$(GC_{pi})$ = internal pressure coefficient from Table 26.11-1.

The wall pressure coefficient ($C_p$) is chosen based on the length-to-width ratio, L/B. The roof pressure coefficient ($C_p$) is chosen based on the mean roof height-to-length ratio, h/L. The mean roof height (h) is the sum of the wall roof height and half the vertical roof height. Interpolation is used to evaluate the coefficient value for all values of L/B, h/L and the roof angle (θ) as shown in Table 2 and 3.

**Table 2: Wall pressure coefficients extracted from Figure 27.4-1 of ASCE 7-10**

| Wall Pressure Coefficients, $C_p$ | | | |
|---|---|---|---|
| **Surface** | **L/B** | **$C_p$** | **Use With** |
| Windward Wall | All values | 0.8 | $q_z$ |
| Leeward Wall | 0-1 | -0.5 | $q_h$ |
| | 2 | -0.3 | |
| | ≥4 | -0.2 | |
| Side Wall | All values | -0.7 | $q_h$ |

**Table 3: Roof pressure coefficients extracted from Figure 27.4-1 of ASCE 7-10**

<table>
<tr><th colspan="12">Roof Pressure Coefficients, $C_p$, for use with $q_h$</th></tr>
<tr><th rowspan="3">Wind Direction</th><th colspan="9">Windward</th><th colspan="3">Leeward</th></tr>
<tr><th colspan="9">Angle, θ (degrees)</th><th colspan="3">Angle, θ (degrees)</th></tr>
<tr><th>h/L</th><th>10</th><th>15</th><th>20</th><th>25</th><th>30</th><th>35</th><th>45</th><th>≥60#</th><th>10</th><th>15</th><th>≥20</th></tr>
<tr><td rowspan="3">Normal to ridge for θ ≥ 10°</td><td>≤0.25</td><td>-0.7<br>-0.18</td><td>-0.5<br>0.0*</td><td>-0.3<br>0.2</td><td>-0.2<br>0.3</td><td>-0.2<br>0.3</td><td>0.0*<br>0.4</td><td>0.4</td><td>0.01 θ</td><td>-0.3</td><td>-0.5</td><td>-0.6</td></tr>
<tr><td>0.5</td><td>-0.9<br>-0.18</td><td>-0.7<br>-0.18</td><td>-0.4<br>0.0*</td><td>-0.3<br>0.2</td><td>-0.2<br>0.2</td><td>-0.2<br>0.3</td><td>0.0*<br>0.4</td><td>0.01 θ</td><td>-0.5</td><td>-0.5</td><td>-0.6</td></tr>
<tr><td>≥1.0</td><td>-1.3**<br>-0.18</td><td>-1.0<br>-0.18</td><td>-0.7<br>-0.18</td><td>-0.5<br>0.0*</td><td>-0.3<br>0.2</td><td>-0.2<br>0.2</td><td>0.0*<br>0.3</td><td>0.01 θ</td><td>-0.7</td><td>-0.6</td><td>-0.6</td></tr>
<tr><td rowspan="5">Normal to ridge for θ < 10 and Parallel to ridge for all θ</td><td rowspan="4">≤ 0.5</td><td colspan="3">Horiz distance from windward edge</td><td colspan="2">$C_p$</td><td colspan="4" rowspan="4">*Value is provided for interpolation purposes.<br><br>**Value can be reduced linearly with area over which it is applicable as follows</td></tr>
<tr><td colspan="3">0 to h/2</td><td colspan="2">-0.9, -0.18</td></tr>
<tr><td colspan="3">h/2 to h</td><td colspan="2">-0.9, -0.18</td></tr>
<tr><td colspan="3">h to 2 h</td><td colspan="2">-0.5, -0.18</td></tr>
<tr><td rowspan="2">≥ 1.0</td><td colspan="3">> 2h</td><td colspan="2">-0.3, -0.18</td><td colspan="2">Area (sq ft)</td><td colspan="2">Reduction Factor</td></tr>
<tr><td colspan="3" rowspan="2">0 to h/2</td><td colspan="2" rowspan="2">-1.3**, -0.18</td><td colspan="2">≤ 100 (9.3 sq m)</td><td colspan="2">1.0</td></tr>
<tr><td colspan="3">> h/2</td><td colspan="2">-0.7, -0.18</td><td colspan="2">250 (23.2 sq m)<br>≥ 1000 (92.9 sq m)</td><td colspan="2">0.9<br>0.8</td></tr>
</table>

As seen in Table 3, the code provides two values for the roof pressure coefficient, Cp. Also, two values are defined for the internal pressure coefficient, GCpi. Finally, two wind orientations, parallel and perpendicular to the ridge, are considered. As a result, a total of eight wind load cases are considered. The flowchart shown in Figure 4 explains how the eight wind load cases are formed. Two major cases of wind loading conditions: wind flowing in the normal direction (along Y-axis) and parallel direction (along X-axis) to the ridge of the tent. These divisions of wind loading cases have two other subdivisions which is due to positive and negative roof pressure coefficients. Each of this subdivision has another two divisions, which is caused by positive and negative values of internal pressure coefficients.

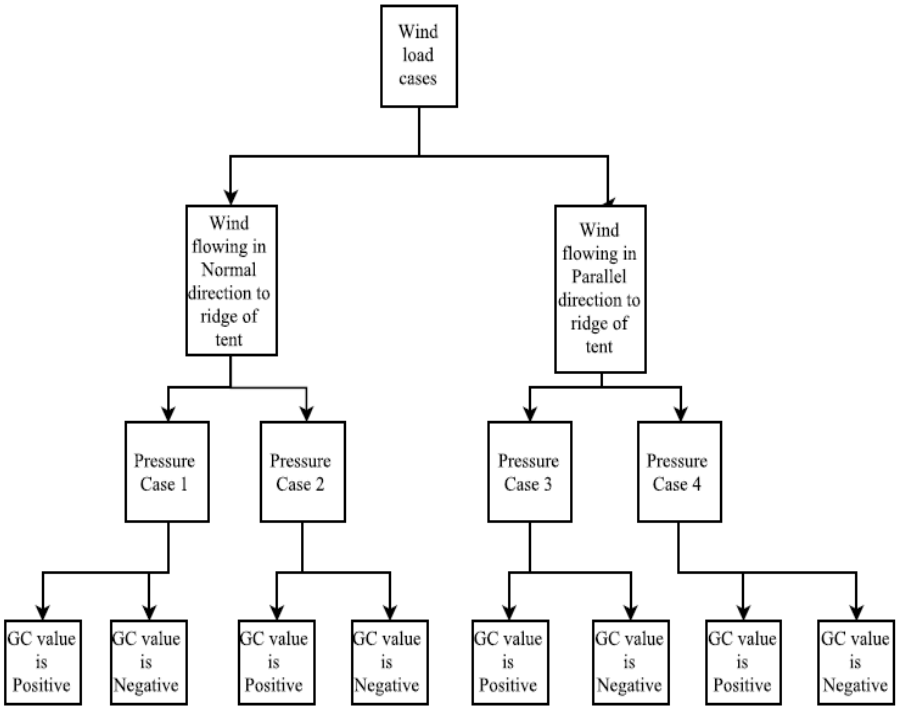


**Figure 4: Flowchart with different wind load conditions**

# CHAPTER THREE

# METHODOLOGY, ALGORITHM AND PROGRAM

## 3.1 FEA: In house MATLAB program and ABAQUS

Hinton and Owen [19] described FEA as a numerical technique for the solving partial differential equations subject to known boundary and initial conditions. In recent years, FEA has been used extensively as a solution technique for many advanced engineering problems.

Per the authors mentioned above, the basic steps involved in the development of a typical finite element computational model for the analysis of a tent are given below.

- The first step is to define the geometry of the frame structure as a set of connected linear segments.
- The structure is then divided into a mesh of finite elements. In this research, conventional two-node linear beam elements are used.
- The system is assumed to be in static equilibrium, i.e., does not vary with time.
- The stiffness matrix '$K^{(e)}$' and the load vector '$f^{(e)}$' for each finite element are calculated and integrated together into a comprehensive stiffness matrix 'K' and load vector 'f' based on the element connectivity.
- The boundary conditions are then applied by removing the rows and columns of 'K' and 'f' corresponding to the constrained degrees of freedom. In this research, the footings of all uprights are assumed to be fixed to the ground. Also, the guys' attachment points to ballasts are assumed to be fixed to the ground as pinned connections.

- The static equilibrium equation ‘Ka = f’, where ‘a’ is the displacement vector of all nodes, is solved for ‘a’ by inverting the global matrix ‘K’.
- After evaluating ‘a’, the reaction at nodes, stresses, strains of elements may be evaluated, as well as the reaction forces in all guy lines.

At the beginning of this project, an in-house FEA script programmed in Matlab was used to conduct the analysis. It was fast and convenient since the whole process was done within the Matlab environment. However, this existing Matlab FEA software did not have the ability to model the non-symmetrical elastic behavior of the guy lines’ material. More specifically, the guy lines are supposed to work in tension but not in compression. This means that the material stiffness should be response-dependent, i.e., non-zero under tensile deformation and zero under compressive deformation. In practice, the guy lines that are on the windward side of the tent are usually in tension and the guy lines that are on the leeward side of the tent are generally loose and slack and does not contribute to the stability of the tent. Since this nonlinear behavior of the guy lines’ material could not be modelled with the in-house Matlab FEA, Abaqus was used as an alternative.

Abaqus [22] is a well-accepted commercial FEA software that has many advanced features, including the ability to model nonlinear behavior of materials. The interface between Matlab and Abaqus is fairly straightforward and does not present any major road block. As mentioned above, Matlab creates the FEA input data file for any given tent design and calls Abaqus to run the analysis and output results. Matlab then reads the output results and post-processes the information.

Note that the FEA analysis used in this research is slightly more complicated than a simple static analysis. It includes multiple steps with one FEA in each step in order to apply the desired pre-tension of the guy lines. This is due to the fact that applying a pre-tension corresponds to reducing the length of the guy lines until the desired pre-tension value is achieved. Since this process is response-dependent, it must be done in several steps. This process is described in Section 3.4.

### 3.2 Description of tent FEA model

Four tent configurations, represented in Figure 5, are considered in this research. The first configuration is a simple tent with a gable roof along the entire length of the tent. This means that the roof has two sides sloped at a desired angle. The second configuration has a hip roof, which has all four sides sloped at a desired angle. In this case, the roof pitch corresponds to the angle of the two roof planes that are parallel to the length of the tent. The angle of the other two roof places is generally not a dependent variable and is therefore not part of the discussion. The third configuration has intermediate posts between the exterior posts and has a gable roof. Finally, the fourth configuration has intermediate posts and a hip roof.

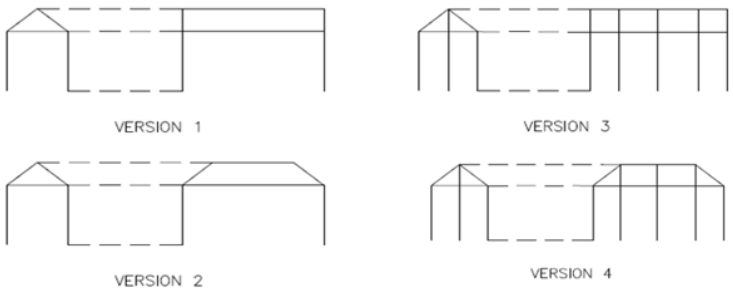


**Figure 5: Different tent configurations**

For the finite element model, the frame of the tent is discretized into nodes and elements. Note that the fabric is not included in the numerical model since it is assumed to have a negligible effect on the mechanical behavior of the tent and on the ballast weights. The nodes and elements are identified using different numbers as shown in Figure 6 and 7. The frame is modeled using beam elements capable of transferring moments. The properties of the beams elements are the cross-sectional area and moment of inertia, Young's modulus of elasticity, and Poisson's ratio. Figures 6 and 7 shows the beam elements in blue and the model include four element per bar of the frame. The guy lines are modeled using a single truss element for each line shown in red in Figures 6 and 7. The properties of the truss elements are the cross-sectional area, Young's modulus of elasticity in tension only (i.e., no compression) and Poisson's ratio. The connections at each end of the truss elements are pinned connections allowing full rotation.

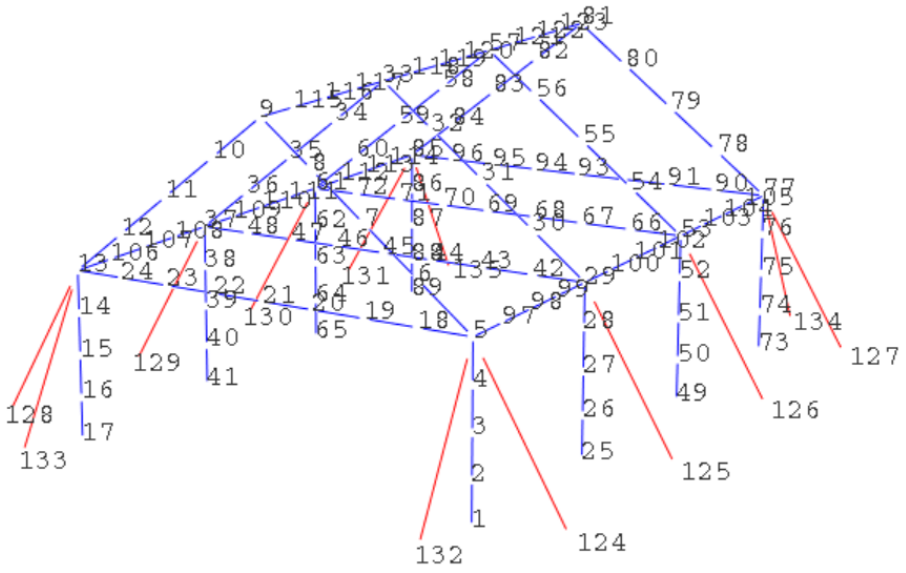


**Figure 6: Tent with node labels**

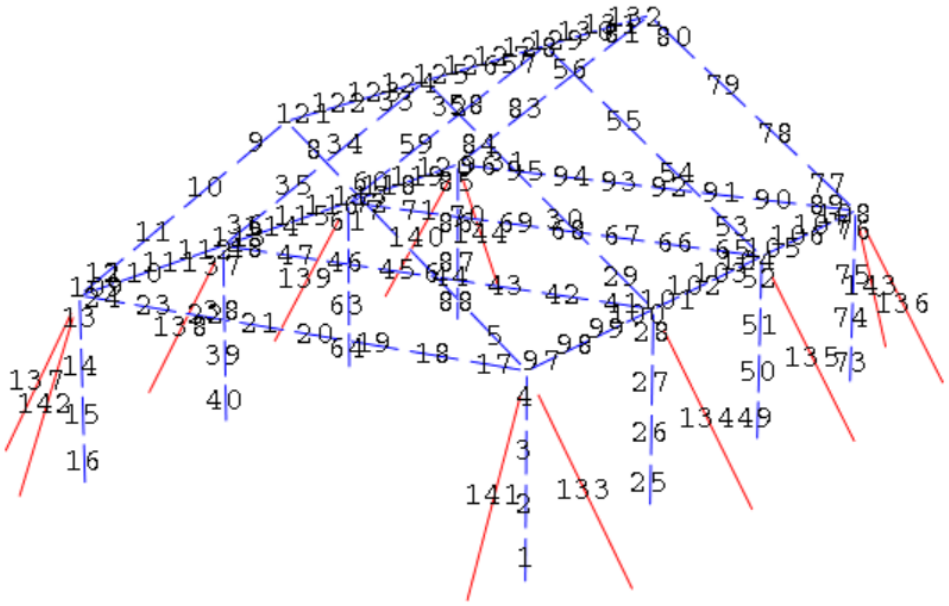

**Figure 7: Tent with element labels (beam and truss elements are shown in blue and red, respectively)**

### 3.3 How surface wind loads are converted to nodal loads

As described in Chapter 2, the wind pressure for a given section of the tent, such as a wall or a roof panel, is calculated based on the formulas and parametric tables provided by code. The total force applied on a section is obtained by multiplying the wind pressure by the surface area of the section. For instance, consider the wall section running along x-axis as shown in Figure 8. The wall section is divided into three sub-sections because it has two intermediate posts running between the exterior posts. As a result, the total force applied on the wall is divided by the number of sub-sections. The resulting force must then be transferred to the corner nodes of each sub-section as shown in Figure 9.

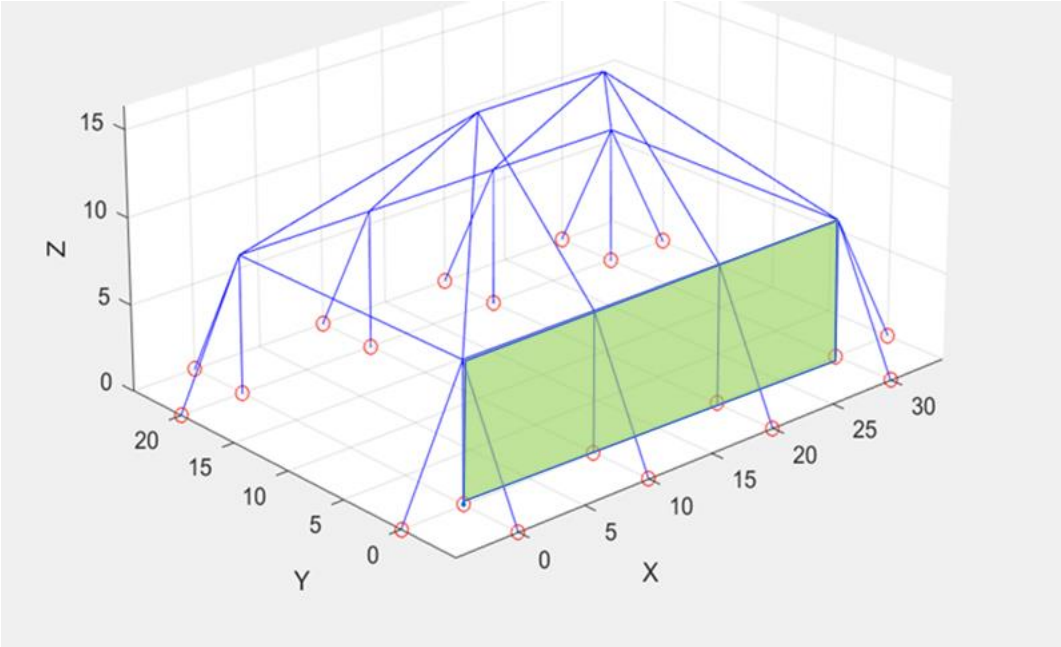


**Figure 8: Tent wall denoted by color 'green'**

According to the color coding of Figure 9, assuming that the wind pressure is uniform on the entire wall, the four nodes of each sub-section has the same nodal force. As a result, the nodes that are common to two adjacent sub-section has the twice as much force as the nodes of a single sub-section, such as the nodes of the exterior posts. As an example, assuming that the force applied on each section is 'F', consider the red-circled arrow, this node has a force of value 'F/4' because the force is equally divided among the four nodes. Considering the interior nodes, the node with the black-circled arrow has a force of value 'F/2' since it has the contribution of the two adjacent sub-sections colored in green and orange (i.e., 'F/4' + 'F/4'). A similar approach was taken for assigning forces to the roof. Roof forces included horizontal and vertical components as shown in Figure 10.

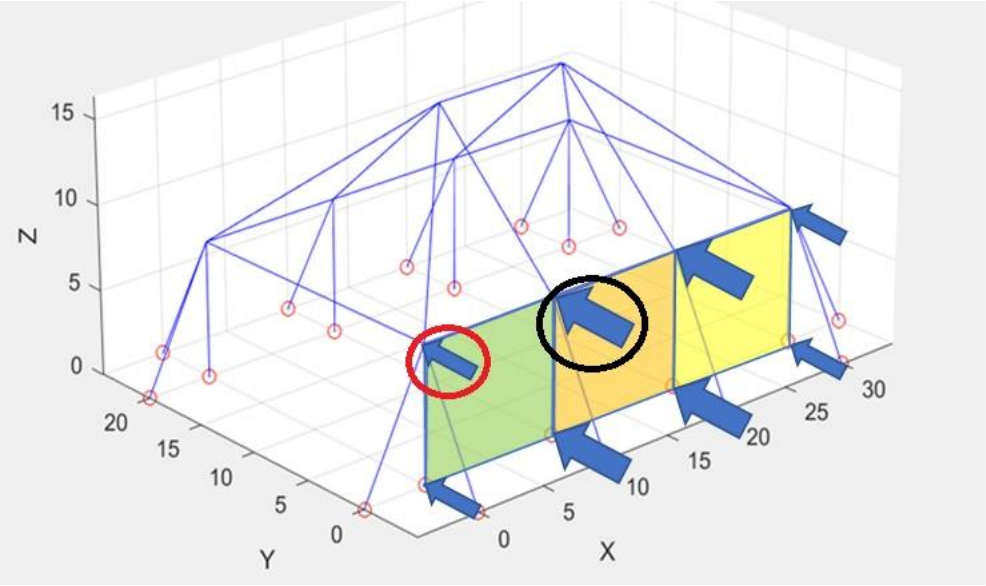


**Figure 9: Different wall sections with nodal forces acting on nodes**

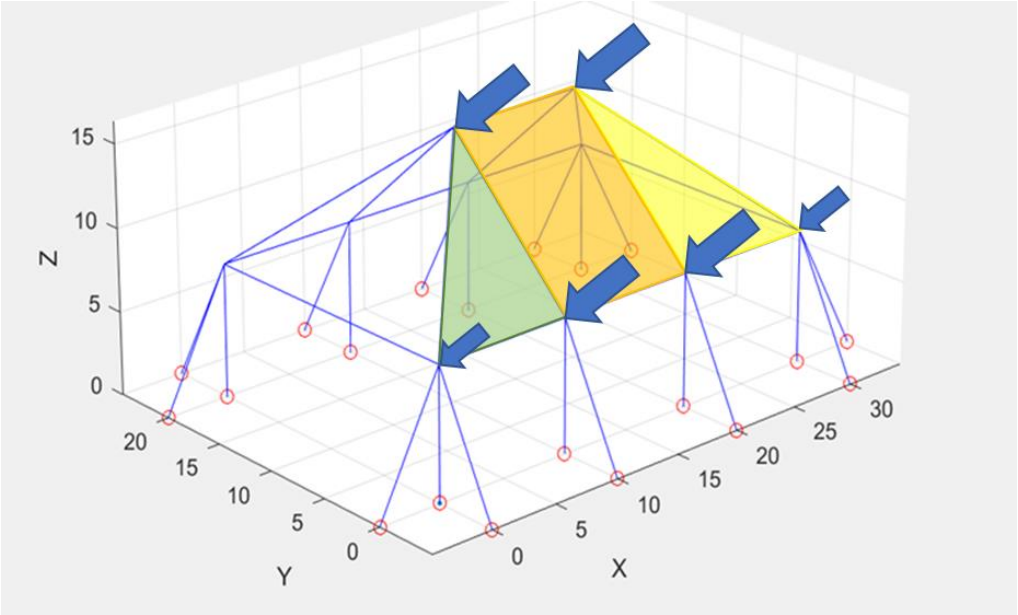


**Figure 10: Different roof sections with nodal forces acting on nodes**

### 3.4 Boundary conditions

Consider the nodes highlighted in red in Figure 11. These nodes are referred to as ground nodes and they are either the endpoints of posts or guys. These are the nodes where

pin boundary conditions are applied. The pin boundary condition means that the three translational degrees of freedom are fixed. Several points need to be made concerning these nodes.

First, the ground nodes of the posts, also referred to as footings, are supposed to be in friction contact with the ground. This means that the nodes are supposed to be able to slide if the horizontal force is sufficiently large. In this research, however, this behavior is neglected as it is assumed to have negligible effect on the ballast weights. The ground nodes of the posts are also supposed to be able to lift off the ground in the case of an upward vertical force. This behavior is modeled using the "No Tension" option of Abaqus for the elements connected to the ground nodes of all posts. The "No Tension" option means that the element has non-zero stiffness in compression by zero stiffness in tension, which is intended to represent the ability of the post to lift off the ground as it would not resist to the tensile force in the post.

It should be noted that an unresolved issue is reducing the accuracy of the results obtained by this research. The "No Tension" option allows simulating the tent's behavior accurately but only in the case where no pre-tension is applied. With pre-tension, the Abaqus solver is not able to converge numerically. Therefore, either the footings of the frame are allowed to lift off but no pre-tension is defined, or the footings are not allowed to lift off but pre-tension can be defined. For the remainder of this thesis, the latter case is considered since it is assumed that pre-tension has more effect on the ballast weights than the ability of the footings to lift off the ground.

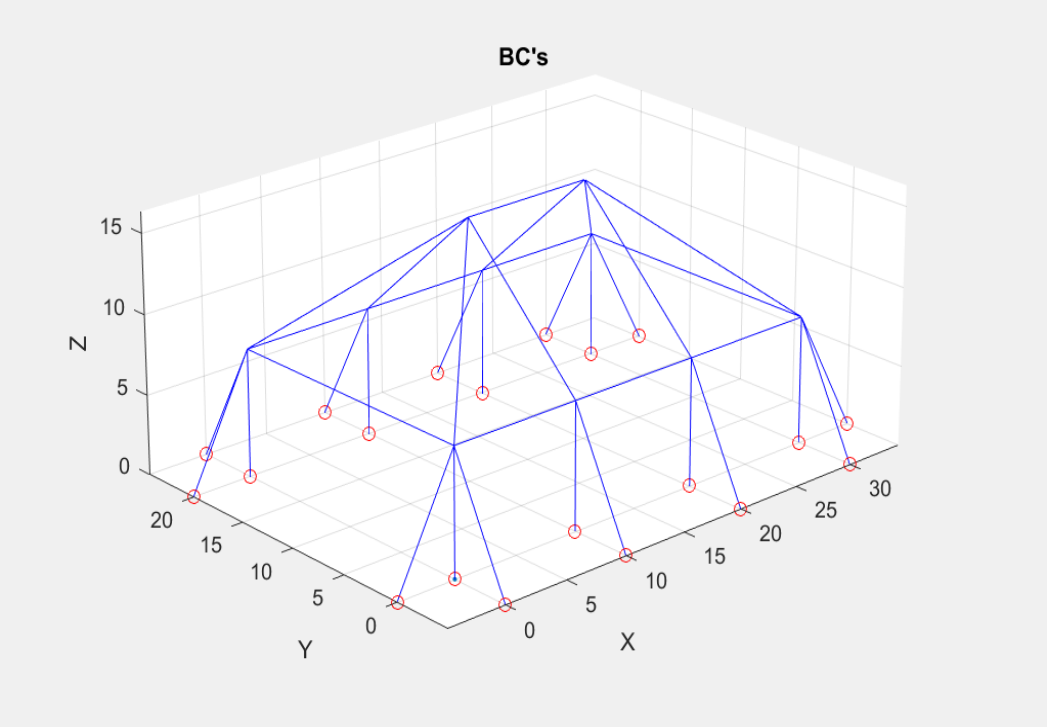


**Figure 11: Tent model showing nodes with pinned Boundary Conditions (BC's)**

Concerning the ground nodes of each guy line, as explained in Chapter 4, the ballasts are not physically modeled. Instead, the guy lines are assumed to go from the top of a post (i.e., eave of the tent) to the ground with a pin boundary condition at the ground.

### 3.5 Application of guy pre-tension

As mentioned in section 3.1, the FEA static analysis using Abaqus includes several steps in order to apply the desired pre-tension in each guy connecting the frame of tent and ballast on the ground. The flowchart shown in Figure 12 explains how the various Matlab scripts interact with each other in a sequence of steps and iterations to return the pre-tensioned guy lines and the reaction forces.

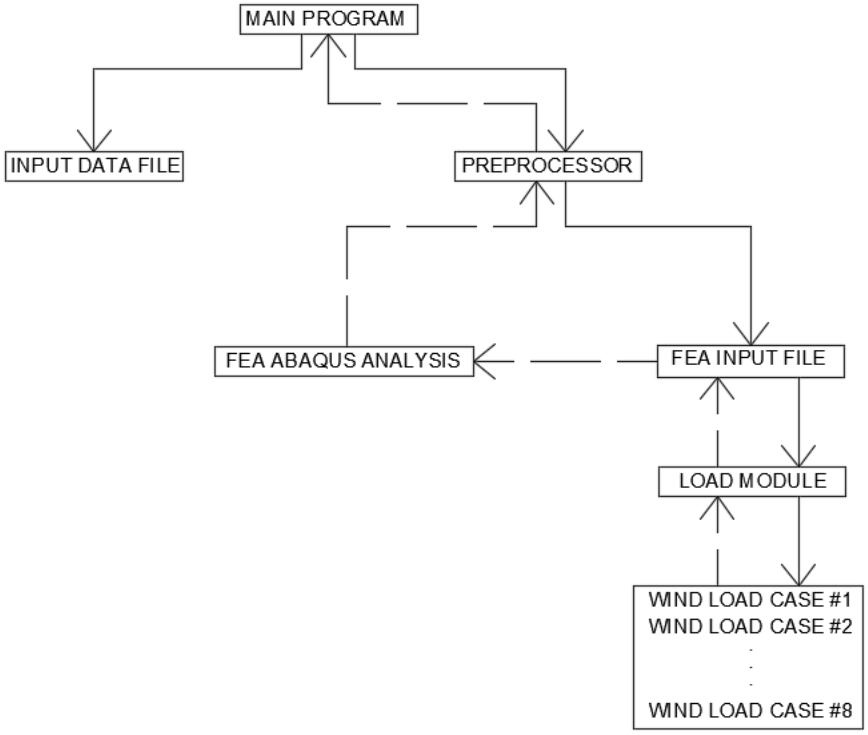


**Figure 12: Flowchart showing the sequence of Matlab scripts and Abaqus**

The different design parameters are obtained by the 'Main Program' from the 'input data file' and these parameter values are used in turn by the 'Preprocessor'. The 'Preprocessor' creates the 'FEA input file' with the input from the 'Load module' which has the path to all possible wind load configurations.

In the flowchart, the 'Load Module' interacts with one of the configurations – 'Wind Load Case #1' to apply one loading configuration out of the eight possible loading configurations available. In this particular case - 'Wind Load Case #1', corresponds to a partially enclosed building condition with wind flowing in the direction parallel to the ridge of the tent and with a $GC_{pi}$ value of +0.55. For each trial containing a new dataset of

parameter values, the ‘FEA Input File’ is updated with a new set of nodes, elements, properties, boundary conditions, and forces.

In the model, the pre-tension of a guy line is achieved by applying a displacement boundary condition that corresponds to translating the ground node of the guy line into the ground in the direction parallel to the guy line. This is exactly equivalent to reducing the length of the guy line to tension it. The issue is that the amount of displacement is a priori unknown since it depends on the position of the guy line, the stiffness of the guy line’s material, and the overall stiffness. This is the reason why the pre-tension is applied using several steps.

The guys are divided into several groups based on position and symmetry. In the case of a tent with two intermediate posts in length and none in width, as shown in Figure 13, there are three groups of guys. They are (1) the guys at corners in longitudinal direction (shown in green), (2) the guys at corners in transversal direction (shown in red), and (3) the intermediate guys between corners in transversal direction (shown in blue) as shown in Figure 13.

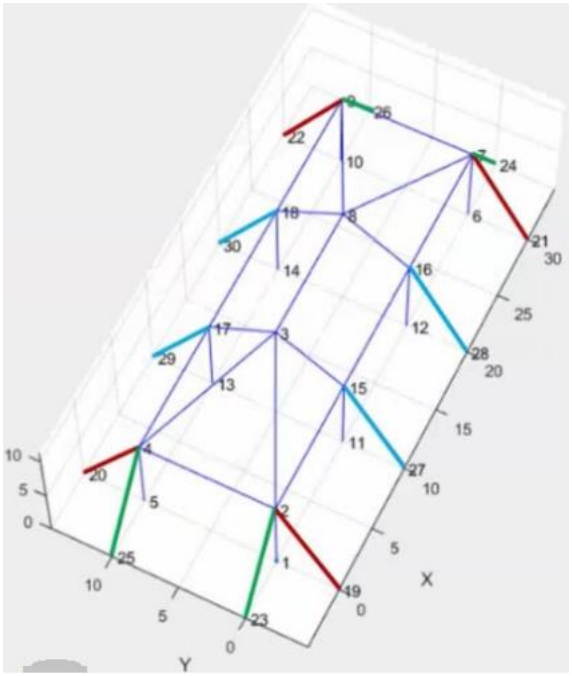


**Figure 13: Guys with same color code to explain symmetry**

All guys in a group behave the same way when it comes to applying the pre-tension without any wind load. This means that all guy lines of a group are subjected to the same displacement boundary condition. In this research, the amount of displacement is approximated based exclusively on the stiffness of the guy line's material. In theory, it should also be based on the stiffness of the frame but the method is too complex and not yet implemented. The approximation of the method induces a small error as long as the stiffness of the guy lines is significantly smaller than the overall stiffness of the frame, which is usually the case.

The equation used to determine the displacement of the guy's ground nodes is based on Hooke's law, which relates the longitudinal stress and strain of a bar defined by it's modulus of elasticity:

$$\delta = TL/(EA) \qquad (3)$$

where

$\delta$ is the downward displacement applied at the guy's ground node in the direction of the guy,

T is the desired pre-tension of the guy line,

L is the undeformed length of the guy line,

E is Young's modulus of elasticity of the guy line's material, and

A is the cross-sectional area of the guy line.For instance, if the tent height is 8 feet and the guy angle is 60 degrees, the length is L = 9.24 ft. If the guy line's material is a polymeric strap of cross-sectional area A = 0.021 $ft^2$ and modulus of elasticity E = 2.1e8 $lbf/ft^2$, assuming that the desired pre-tension is T = 300 lbf, the required displacement is $\delta$ = 300*9.24/0.021/2.1e8 = 6.29e-4 ft. When applying this displacement of the ground node of each guy of a given group, the actual tension ends up being about 292 lbs, which is close enough to the desired pre-tension of 300 lbf.

After pre-tensioning the guys, the 'main program' interacts with the 'FEA Abaqus Analysis' to calculate the actual pre-tension and verify that it is close enough to the desired value for each guy line. The wind loads are then applied and the reaction forces are calculated by the FEA for all ground nodes, including the ground nodes of the guy lines and the ground nodes of the posts. At the end of this procedure, an output file is created with displacement of all nodes and the three components of the reaction forces. This file is then used to calculate the heaviest ballast weight for the worst wind loading configuration.

# CHAPTER FOUR

# CALCULATION OF BALLAST WEIGHT

## 4.1 Ballast configurations and their failure modes

In this research, it is assumed that the guy line is always attached to the top at the center of the ballast. Three failure modes are considered – ballast sliding, tilting, and lift. The equations used to find the minimum ballast weight to prevent each of the three failure modes are given below.

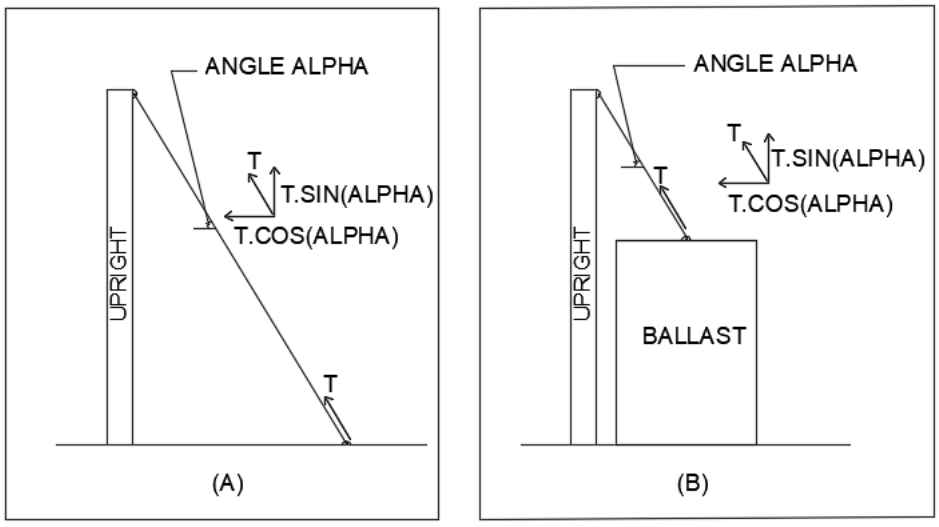


**Figure 14: (A) Guy connecting upright and ground – Numerical Model**
**(B) Guy connecting upright and ballast – In reality**

### 4.1.1 Ballast sliding

Consider the free body diagram (shown in Figure 15) at the failure point, which corresponds to the onset of sliding. 'T' is the tension of the guy, 'α' is the angle between the guy and the horizontal, 'd', 'h', and 'W' are the width, height, and weight of the ballast, respectively, N is the vertical reaction from the ground, and '$F_f$' is the friction force at the bottom of the ballast.

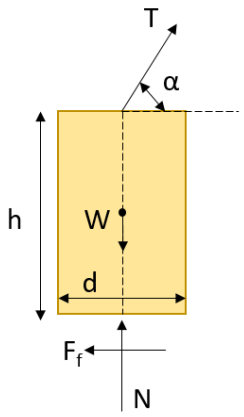


**Figure 15: Free body diagram of the ballast due to sliding**

The tension of the guy can be resolved into horizontal and vertical components Tcos(α) and Tsin(α). At the onset of sliding, the frictional force is equal to the sum of vertical forces multiplied by the load factor and considering static equilibrium, the sum of all horizontal forces must be equal to zero,

$$N - W + T\sin(\alpha) = 0 \quad (4)$$

$$F_f - \mu N = 0 \quad (5)$$

$$F_f = \mu\,[W - T\sin(\alpha)] \quad (6)$$

$$F_f - [T\cos(\alpha)] = 0 \quad (7)$$

Solving for the ballast weight 'W' using the above last two equations, the weight of ballast is derived as,

$$W = [T\cos(\alpha) / \mu] + [T\sin(\alpha)] \quad (8)$$

The weight of the ballast '$W_i$' (to be decided by the tent installer) should always be greater than the theoretical ballast weight 'W' to avoid sliding.

### 4.1.2 Ballast tilting

For this failure mode, it is assumed that the ballast is about the tilt and rotate about the leading edge of the ballast's bottom plane in contact with the ground. In this case, most of the friction between the ballast and the ground is concentrated at the leading edge of the ballast. Therefore, it is assumed that the vertical reaction of the ground under the ballast is applied at the edge of the ballast as shown in Figure 16. This assumption is conservative and corresponds to the worst-case scenario since in reality the reaction forces N and $H_f$ should be somewhere between the center and the edge of the ballast.

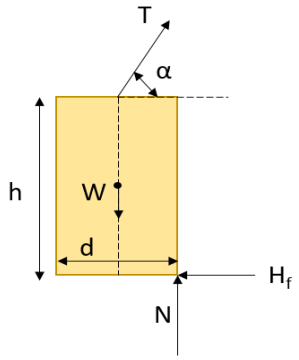


**Figure 16: Free body diagram of a ballast at the onset of tilting**

At static equilibrium, the sum of vertical forces and horizontal forces are zero,

$$T\cos(\alpha) - H_f = 0 \quad (9)$$

$$T\sin(\alpha) - W + N = 0 \quad (10)$$

Considering the sum of moments about the point at which the ballast tilts,

$$[T\sin(\alpha)](d/2) - W(d/2) + [T\sin(\alpha)](h) = 0 \quad (11)$$

Solving for 'W' using the above three equations, the ballast weight is,

$$W = [T\cos(\alpha)](2h/d) + T\sin(\alpha) \quad (12)$$

The weight of the ballast '$W_i$' (to be decided by the tent installer) should always be greater than 'W' to avoid tilting.

### 4.1.3 Ballast lifting

The last failure mode which needs to be considered is to the vertical lift of the ballast. The weight of the ballast must be greater than the vertical force components of the tension at the top of the ballast. This is explained by the equation,

$$W = T.\sin(\alpha) \tag{13}$$

The weight of the ballast '$W_i$' (to be decided by the tent installer) should always be greater than 'W' to avoid lifting.

## 4.2 Calculating final Ballast Weight

The three failure modes of the ballasts are explained in the previous section. All three kinds of failure are given equal importance and the equation which has the maximum value will be selected by the installer and based on this value, the installer decides the final ballast weight for the guys in question. The three equations of ballast weights are given below,

$$W_1 = [T\cos(\alpha) / \mu] + [T\sin(\alpha)] \tag{14}$$

$$W_2 = [T\cos(\alpha)](2h/d) + T\sin(\alpha) \tag{15}$$

$$W_3 = T\sin(\alpha) \tag{16}$$

$$W_i > \max(W_1, W_2, W_3) \tag{17}$$

The ballast weight '$W_i$' (shown in equation 17) which is to be decided by the installer should always be greater than the maximum of three values.

# CHAPTER FIVE

# RESULTS – GUY TENSION AND REACTION FORCES

## 5.1 Full Factorial Design of Experiments

Design of experiments (DOE) is an analytical method which is used to determine the relationship between factors affecting a process (which can be controllable or uncontrollable) and the output (result) of that process [20]. The factors affecting a process are segregated into controllable and uncontrollable because parameters used in an experiment can be modified or unmodified.

The method adopted in this research is the Full Factorial method which is an exhaustive analysis of all possible cases based on the number of parameters, also referred to as variables, and the number of levels of each parameter.

In this chapter, a total of six main variables are considered. The six variables are length, width, roof pitch angle, number of intermediate posts along the length, number of intermediate posts along the width, and wind speed. The number of intermediate posts along the length and along the width are fixed in this chapter and their values are 2 and 0, respectively. Hence the number of levels are 1 each. The number of levels for each variable are given in table below.

**Table 4: Variables and their number of levels**

| Variable | Values | # of Levels |
|---|---|---|
| Length | 20,30,40 | 3 |
| Width | 10,20,30 | 3 |
| Roof Pitch | 6,8,10 (in 12) | 3 |
| Intermediate posts along Length | 2 | 1 |
| Intermediate posts along Breadth | 0 | 1 |
| Wind Speed | 30,40,50,60,70 | 5 |

After finding the number of levels for each variable, the number of levels are multiplied to estimate the total number of cases.

$$3 \times 3 \times 3 \times 5 \times 1 \times 1 = 135 \text{ cases}$$

To calculate the total time required to calculate all the wind load combinations, it is multiplied by 8.

$$135 \times 8 = 1080 \text{ cases}$$

The time taken to calculate the one case out of 1080 cases is roughly 5 minutes. Hence to obtain the total time for calculating 1080 cases, it is

$$1080 \text{ cases} \times 5 \text{ minutes} = 90 \text{ hours}$$

Thus, it takes approximately 90 hours to calculate the ballast weights for 1080 cases. Since this method showed that conducting experiments was feasible in a reasonable time, the Full Factorial method was adopted to determine the variable configuration cases. The weight of the ballast is directly dependent upon the wind loads applied on the tent structure. One of the important parameters which influences the weight of the ballast is the surface area of the tent. Intuitively, the bigger the tent, the greater the ballast. However, this statement is not always true because of the counter-effect of other parameters such as the number of intermediate posts. For a given length of the tent, the distance between intermediate posts can vary between 10 and 20 feet depending on the length of the tent. The smaller the distance between posts, the more intermediate posts, and therefore the more individual ballasts. Increasing the number of intermediate posts results in decreasing the weight of individual ballasts. Therefore, the length and the number of intermediate posts have opposite effects on individual ballast weights and may cancel each other.

### 5.2 Non-Uniform Distribution of guy tension

In this section, the ballast weight is decided based on three groups of guys instead of having a unique ballast weight for each guy. The pre-tension applied to the guys was assumed to be uniform before the application of wind loads. After the wind loads were applied, the ballast weight varied around the tent for each guy. As per our analysis, node numbers 19, 23 and 27 (shown in Figure 17) were the strategic locations or points where the highest values of ballast weights were obtained. The windward side has the highest and positive coefficients which makes the corners easier to have the heaviest ballast weights. Out of the eight combinations of load cases, the case which had the heaviest ballast weight differed often but in each trial the node number which had heaviest ballast weight was found to be one among these three node numbers – 19, 23 and 27.

**Table 5: Ballast weights and wind load cases for node numbers 19, 23 and 27**

| L (ft) | W (ft) | P (in 12) | Node #19 (lbs) | Node #23 (lbs) | Node #27 (lbs) | Wind case for #19 | Wind case for #23 | Wind case for #27 |
|---|---|---|---|---|---|---|---|---|
| 20 | 10 | 10 | 754.8 | 628.1 | 645.9 | 06 | 04 | 08 |
| 30 | 20 | 6 | 1171 | 1261 | 965.6 | 08 | 04 | 06 |
| 40 | 10 | 8 | 1415 | 613.6 | 1304 | 08 | 04 | 08 |

The above statement which said the heaviest ballasts occurred at node numbers 19, 23 and 27 is explained with the help of ballast weights obtained in Table 5. For a fixed wind speed of 70 mph and with the numbers of intermediate posts along length and width as 2 and 0, the above ballast weights for the corresponding wind load cases were obtained.

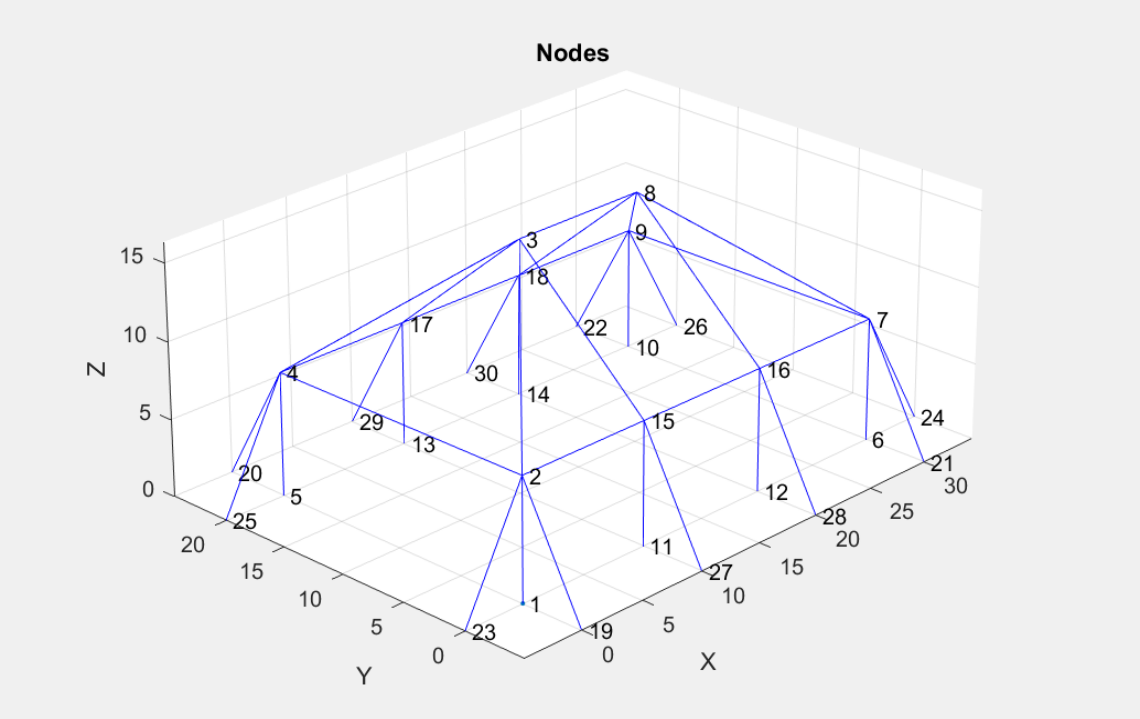


**Figure 17: Tent with 'nodes' marked by numbers**

The heaviest ballast occurred either at node number 19 or node number 23 as shown in rows 1 and 2 of Table 5. For a few trials, the ballast weight at node number 27 was higher than the ballast weight at node number 23 as shown in row 3 of Table 5 and the reason this happened was because of the forces acting on node 15 was greater than the forces acting on node 2 in the transversal direction due to large pressure coefficients ($C_p$) and large tributary width of the forces acting on node 15.

The heaviest ballasts are needed at the node numbers 19, 23 and 27. This represents the corner of the tent. If the wind is to blow on either longitudinal or transversal direction on any side of the wall, the tent will have the corners as the critical areas which have the heaviest ballast weights by symmetry. This leads to three groups of guys which are explained by color code in Figure 13. The three types of guys based on position are – guys

at corners in longitudinal direction (shown in green), guys at corners in transversal direction (shown in red) and intermediate guys between corners in transversal direction (shown in blue). Thus, a tent with this configuration will have three groups of ballast weights with each ballast weight corresponding to each type of guy based on position.

In the following sections, the effect of each individual parameter on the maximum ballast weight is studied. The effects of two simultaneous parameters is then considered to show the mutual effect on ballast weights. For instance, the length of the tent is considered while maintaining all other parameters constant. Then, the length of the tent and the number of intermediate posts are considered simultaneously.

### 5.3 Effect of Tent Length

The first parameter considered was the length of the tent. The length of the tent examined were 20 ft, 30 ft and 40 ft. The rest of the parameters, including the number of intermediate posts, were kept constant and those considered are listed in Table 6.

**Table 6: Parameter values used for different values of length**

| | |
|---|---|
| Length of tent | Varies |
| Width of tent | 10 ft |
| Pitch of roof | 6 in 12 |
| Intermediate posts along length | 2 |
| Intermediate posts along width | 0 |
| Speed of wind | 70 mph |

The pre-tension was restricted to 300 lbf for all the guys connecting the frame and ballasts. As shown in Figure 18, the maximum ballast weight increases proportionally with the length. The maximum ballast weights were found to be 673.7 lbs, 1001 lbs and 1335 lbs for lengths 20 ft, 30 ft and 40 ft respectively.

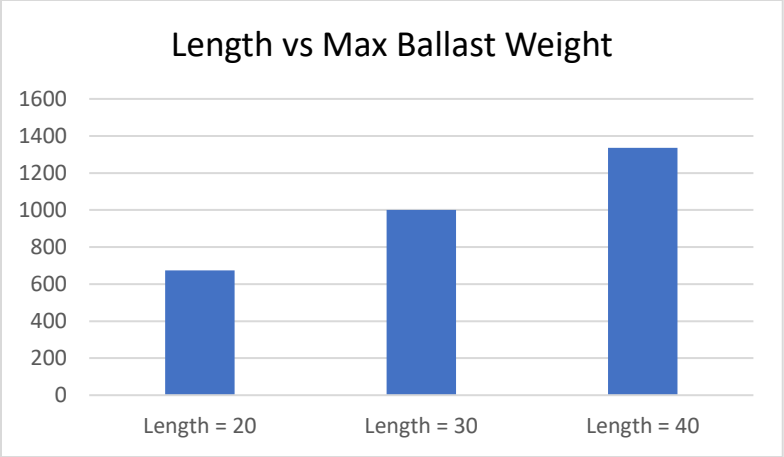


**Figure 18: Graph showing length of tent (ft)(X-axis) vs. ballast weights (lbs)(Y-axis)**

### 5.4 Effect of Tent Width

The second parameter considered was the width of the tent. The width of the tent examined were 10 ft, 20 ft and 30 ft. The rest of the parameters were kept constant and those considered are listed in Table 7.

**Table 7: Parameter values used for different values of width**

| | |
|---|---|
| Length of tent | 40 ft |
| Width of tent | Varies |
| Pitch of roof | 6 in 12 |
| Intermediate posts along length | 2 |
| Intermediate posts along width | 0 |
| Speed of wind | 70 mph |

The pre-tension was restricted to 300 lbf for all the guys connecting the frame and ballasts. As envisioned, the ballast weight increases in the same way as the parameter value increases for tent width. In the below Figure 19, the corresponding ballast weights for widths 10 ft, 20 ft and 30 ft were found to be 1335 lbs, 1692 lbs and 2264 lbs.

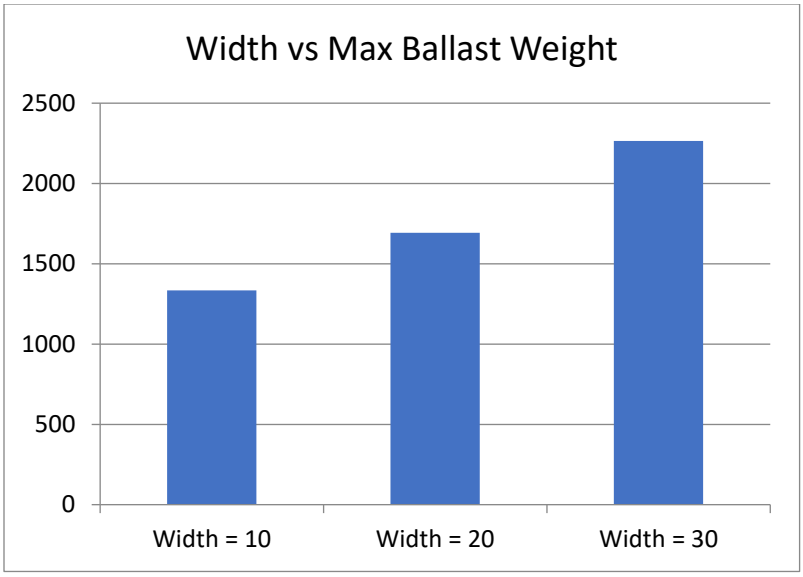


**Figure 19: Graph showing width of tent (ft)(X-axis) vs. ballast weights (lbs)(Y-axis)**

### 5.5 Effect of Roof Pitch Angle

The third parameter considered was the roof pitch angle of the tent. The roof pitch of the tent examined were 6 (in 12), 8 (in 12) and 10 (in 12). The rest of the parameters were kept constant and those considered are listed in Table 8.

**Table 8: Parameter values used for different values of roof pitch angle**

| | |
|---|---|
| Length of tent | 30 ft |
| Width of tent | 20 ft |
| Pitch of roof | Varies |
| Intermediate posts along length | 2 |
| Intermediate posts along width | 0 |
| Speed of wind | 70 mph |

The pre-tension was restricted to 300 lbf for all the guys connecting the frame and ballasts. As predicted, the ballast weight increases in the same way as the parameter increases from a small value to big value. In the below table, the corresponding ballast

weights for roof pitches 6 (in 12), 8 (in 12) and 10 (in 12) were 1261 lbs, 1426 lbs and 1684 lbs.

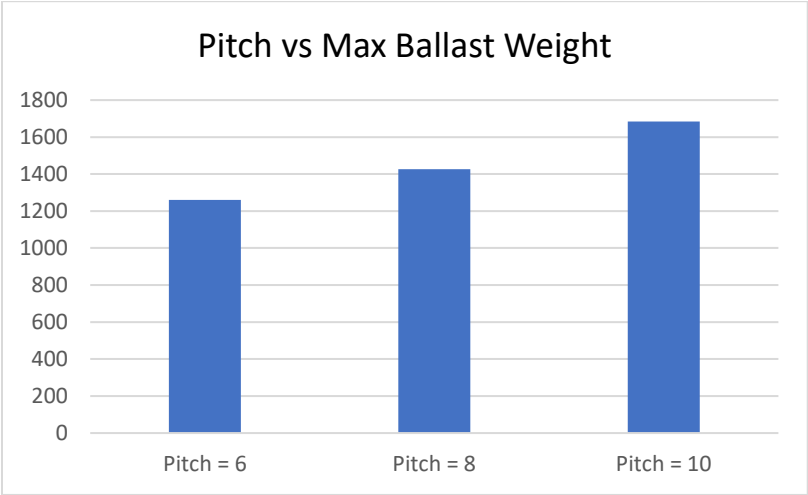


**Figure 20: Graph of pitch angle in tent roof (per 12 inches)(X-axis) vs. ballast weights (lbs)(Y-axis)**

### 5.6 Effect of Speed of Wind

The fourth parameter considered was the wind speed. The wind speed acting on tent examined were 30 mph, 40 mph, 50 mph, 60 mph and 70 mph. The rest of the parameters were kept constant and those considered are listed below.

**Table 9: Parameter values used for different values of wind speeds**

| | |
|---|---|
| Length of tent | 30 ft |
| Width of tent | 20 ft |
| Pitch of roof | 6 in 12 |
| Intermediate posts along length | 2 |
| Intermediate posts along width | 0 |
| Speed of wind | Varies |

The pre-tension was restricted to 300 lbf for all the guys connecting the frame and ballasts. As anticipated, the ballast weight increases in the same way as the parameter

increases from a small value to big value. As shown in Figure 21, the corresponding ballast weights for wind speeds 30 mph, 40 mph, 50 mph, 60 mph and 70 mph were 402.4 lbs, 502.8 lbs, 644.1 lbs, 926.8 lbs and 1261 lbs.

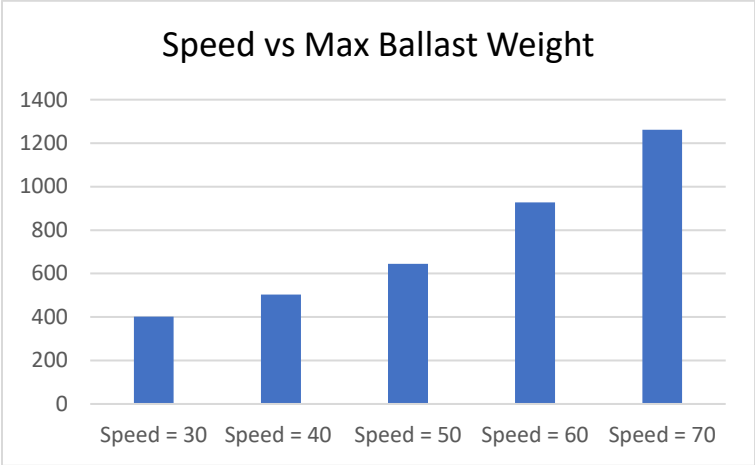


**Figure 21: Graph showing wind speeds (mph)(X-axis) vs. ballast weights (lbs)(Y-axis)**

### 5.7 Effect of Frame Stiffness

A secondary parameter considered was frame stiffness. The radius of the frame elements used for different iteration was different. If a standard value was taken, such as R, the rest of the values taken were R/10, R/2, R*2 and R*10. The rest of the parameters were kept constant and those considered are listed in Table 10.

**Table 10: Parameter values used for different values of frame stiffness**

| | |
|---|---|
| Length of tent | 30 ft |
| Width of tent | 20 ft |
| Pitch of roof | 8 in 12 |
| Intermediate posts along length | 2 |
| Intermediate posts along width | 0 |
| Speed of wind | 70 mph |

The pre-tension was restricted to 500 lbf for all the guys connecting the frame and ballasts. The inner and outer radius values used for R were 0.0407 ft and 0.1547 ft. Based on this value, it was multiplied by 2 and 10, followed by dividing this value by 2 and 10. It was seen that as the radius increased, the stiffness increased. With increased stiffness, the ballast weights got reduced. The respective ballast weights for radius values R/10, R/2, R, R*2 and R*10 were 3041 lbs, 2533 lbs, 1138 lbs, 522 lbs, and 433 lbs.

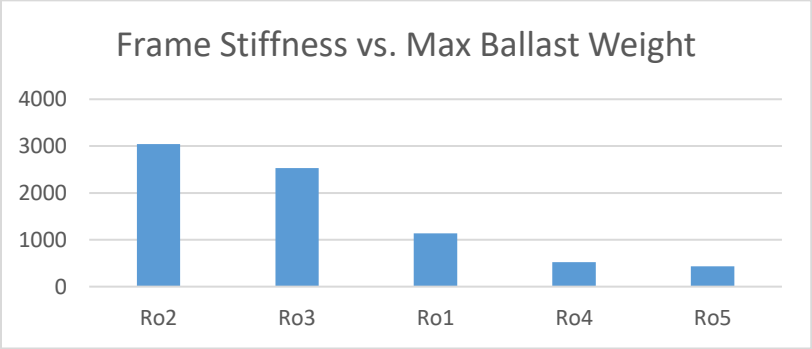


**Figure 22: Graph showing frame stiffness ('R' in inches)(X-axis) vs. ballast weights (lbs)(Y-axis)**

As expected, the stiffer the frame, the more resistance can be provided by the frame. Since the footings are assumed fixed to the ground, the guy lines are less solicited and the ballast weight can be smaller.

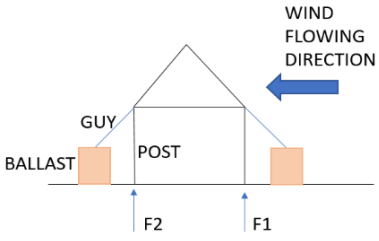


**Figure 23: Reaction forces of the ground to the posts – F1 is windward post & F2 is for leeward post**

When the frame stiffness is considered, uplift forces at the corners are a concern. As shown in Figure 23, F1 & F2 are the reaction forces applied by the ground to the windward and leeward posts, respectively. A positive value of F1 means that the post is being pushed downward into the ground, and a negative value of F1 means that post is being pulled upward and lifted off the ground. Figure 23 shows the reaction forces at the windward and leeward posts for the worst wind load case. This figure clearly shows that the frame stiffness has significant effect on the reaction forces. Also, the reactions that are positive for a frame stiffness value may become negative for another frame stiffness value, which may affect significantly the ballast weights. It can be concluded that the numerical model is valid only when no significant uplift occurs at the post of maximum ballast weight. Note that this issue should be investigated further in the future. For the present time, it is assumed that the frame stiffness is the middle case 'R' where no uplift occurs.

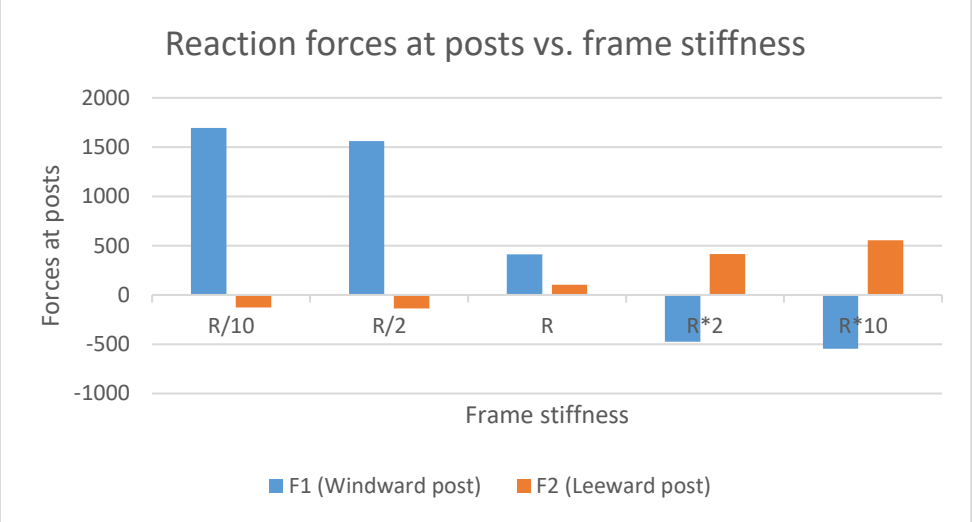


**Figure 24: Forces F1 (lbs)(ground reaction at windward post) and F2 (lbs) (ground reaction at leeward post)**

### 5.8 Effect of Pre-tension

Another secondary parameter considered was the pre-tension. The Pre-tension values considered were between 300 lbf and 1500 lbf. The change in pre-tension was considered for two different lengths (30 ft and 40 ft), widths (10 ft and 20 ft), roof pitches (6 in 12 and 8 in 12) and wind speeds (60 mph and 70 mph). The number of intermediate posts along length was 2 and along width was 0.

#### 5.8.1 Effect of change in length on pre-tension

**Table 11: Ballast weights for different lengths on given pre-tension**

| Prestension | Length = 30 ft | Length = 40 ft |
|---|---|---|
| 300 lbf | 1040 lbs | 1352 lbs |
| 1500 lbf | 1923 lbs | 2141 lbs |

Two different lengths of the tent were considered for different values of pre-tension with fixed values of width = 20 ft, roof pitch = 8 in 12 and wind speed = 70 mph. Comparison of ballast weights for same pre-tension values but different lengths show that there was a substantial difference between the two weights.

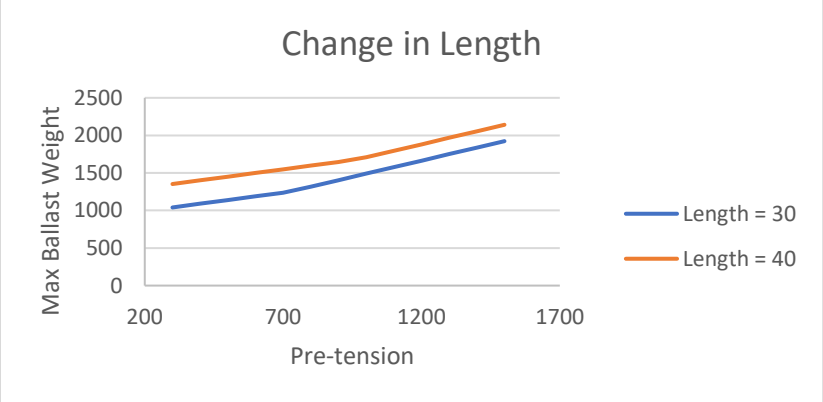


**Figure 25: Graph showing pre-tension (lbf)(X-axis) vs. ballast weights (lbs)(Y-axis) for different lengths (ft)**

### 5.8.2 Effect of change in width on pre-tension

**Table 12: Ballast weights for different widths on given pre-tension**

| Prestension | Width = 10 ft | Width = 20 ft |
|---|---|---|
| 300 lbf | 987.1 lbs | 1040 lbs |
| 1500 lbf | 1902 lbs | 1923 lbs |

Two different widths of the tent were considered for different values of pre-tension with fixed values of length = 30 ft, roof pitch = 8 in 12 and wind speed = 70 mph. Comparison of ballast weights for same pre-tension values but different widths show that there was a small difference between the two weights. This can be attributed to the fact that the difference in tributary area exposed to the wind for two different widths was smaller.


**Figure 26: Graph showing pre-tension (lbf)(X-axis) vs. ballast weights (lbs)(Y-axis) for different widths (ft)**

### 5.8.3 Effect of change in roof pitch on pre-tension

**Table 13: Ballast weights for different roof pitches on given pre-tension**

| Prestension | Pitch = 8 in 12 | Pitch = 10 in 12 |
|---|---|---|
| 300 lbf | 1040 lbs | 1046 lbs |
| 1500 lbf | 1923 lbs | 1927 lbs |

Two different roof pitches of the tent were considered for different values of pre-tension with fixed values of length = 30 ft, width = 20 ft and wind speed = 70 mph. Comparison of ballast weights for same pre-tension values but different roof pitches show that there was negligible difference between the two weights. This can be attributed to the fact that the difference in tributary area exposed to the wind for two different roof pitches was smaller.

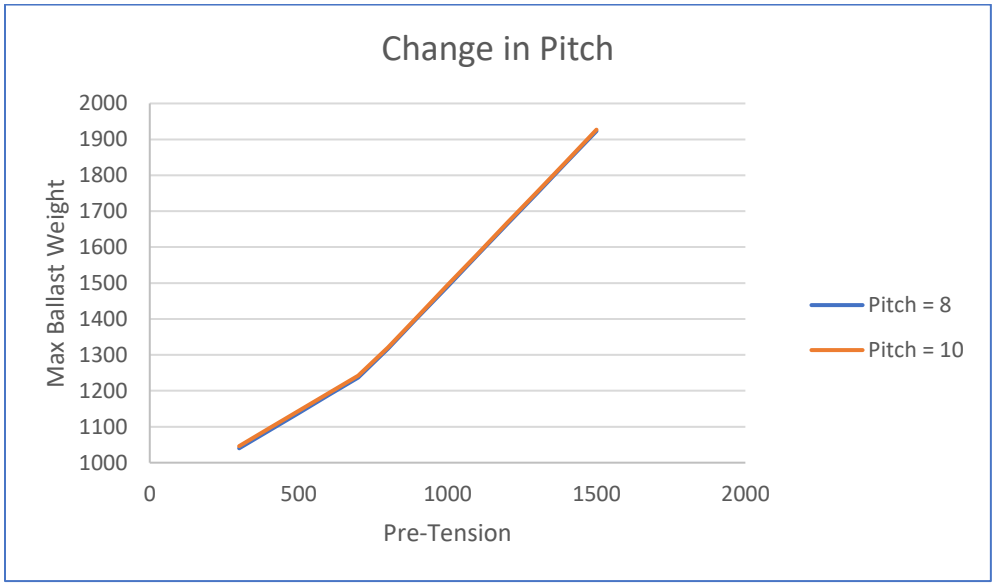


**Figure 27: Graph of pre-tension (lbf)(X-axis) vs. ballast weights (lbs)(Y-axis) for different roof pitches (per 12 inches)**

### 5.8.4 Effect of change in wind speed on pre-tension

**Table 14: Ballast weights for different wind speeds on given pre-tension**

| Pre-tension | Speed = 60 mph | Speed = 70 mph |
|---|---|---|
| 300 lbf | 803.1 lbs | 1040 lbs |
| 1500 lbf | 1758 lbs | 1923 lbs |

Two different wind speeds were considered for different values of pre-tension with fixed values of length = 30 ft, width = 20 ft and roof pitch = 8 in 12. Comparison of ballast weights for the same pre-tension values but different wind speeds show that there was a substantial difference between the two weights. Hence the faster the wind, heavier the ballast weight.

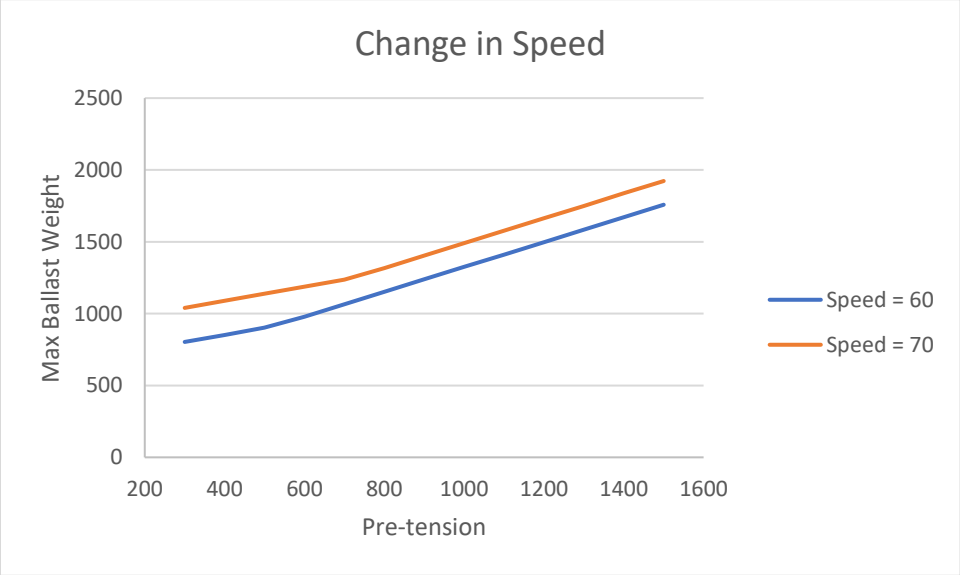


**Figure 28: Graph showing pre-tension (lbf)(X-axis) vs. ballast weights (lbs)(Y-axis) for different wind speeds (mph)**

# CHAPTER SIX

# EXPERIMENTAL MEASUREMENTS

## 6.1 Experimental Setup

Experiments were conducted to determine the load factor. The load factor depends on the type of ballast and ground surface. The type of ballasts which can be used are plastic barrels filled with water or concrete, steel drum filled with concrete, and concrete blocks. The ground surfaces which are used usually are asphalt, smooth concrete, rough concrete, grass, dirt and gravel. Each ground surface can be either wet or dry. Surface modifiers like steel plates and polymeric pads can be used between the ballast and ground surface to potentially increase the overall friction coefficient.

The experimental setup has a guy connecting the ballast at the mid height and the other end of the guy connecting a load cell as shown in Figure 29. Another guy is connecting the winch and the load cell. The winch pulls the guy connecting the load cell which measures the force at which the ballast movement was noted. This scenario is the expected 'failure' of the ballasting system. Only two types of failures were observed: (1) ballast sliding and (2) ballast tilting.

**Table 15: Ballast weights used along with their diameters**

| Ballast | Weight (lbs) | Diameter (in) |
|---|---|---|
| I | 503 | 19 |
| II | 300 | 13.5 |
| III | 181.8 | 19 |

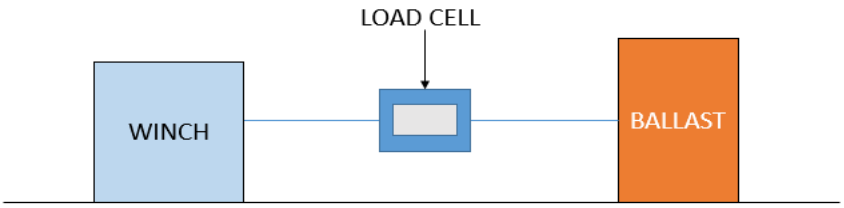


**Figure 29: Experimental setup**

## 6.2 Conversion from guy tension to ballast weight

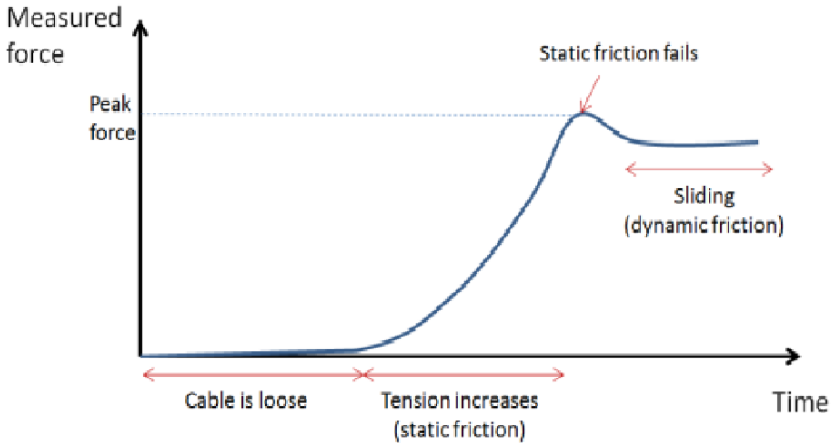


**Figure 30: Force measured on load cell vs. time graph [24]**

The wind loads were applied to the tent structure in simulation which returned the reactions in both horizontal ($RF_h$) and vertical ($RF_v$) directions. The peak force at which the ballast moved or failed was noted by the load cell as shown in Figure 30. The measured force against time graph illustrates how the force increases with time until it reaches a peak value as the ballast was pulled by the winch through the two pulleys. The force declines after the failure point, i.e., after it has reached 'Peak Force'. The same experiment was simulated by the combination of using Matlab and Abaqus software.

The reaction in vertical direction ($RF_v$) is considered as it is, whereas the reaction in horizontal direction ($RF_h$) was divided by the friction coefficient ($\mu$) to get the equivalent force in the vertical direction ($RF_h/\mu$). The ballast weight 'W' value must always be higher than either of the reaction forces $RF_v$ or $RF_h/\mu$ in order to ensure stability of the post.

### 6.3 Determination of Load factors

The experiment was carried out on a dry concrete condition. The aim of this experiment was to determine which ballast was suitable for our future experiments based on the consistency of its friction coefficients or load factors. Five trials were done for two conditions – (1) with one pulley and (2) with two pulleys. Two pulleys were used to record smooth movement of ballasts under sliding failure. The force at which ballast started to slide or tilt was noted. The average force from all five trials were taken and was divided by the ballast weight to obtain friction coefficient. Tables 16 and 17 show that irrespective of using one or two pulleys, the friction coefficients obtained are the same for Ballast type I – the heaviest among the three tested ballasts. A friction coefficient value of 0.23 was recorded for Ballast I.

**Table 16: Friction coefficients for experiments conducted with one pulley**

| Experiment with one pulley | | | | | | | |
|---|---|---|---|---|---|---|---|
| Ballast Type | Trial 1 | Trial 2 | Trial 3 | Trial 4 | Trial 5 | Average (lbs) | Friction coefficient |
| I | 109.2 | 117.05 | 120 | 113.3 | 112.15 | 114.34 | 0.23 |
| II | 85.5 | 86.4 | 81.35 | 84.05 | 82.1 | 83.88 | 0.28 |
| II | 54.25 | 55.95 | 57.4 | 52.15 | 58.7 | 55.69 | 0.31 |

**Table 17: Friction coefficients for experiments conducted with two pulleys**

| Experiment with two pulleys | | | | | | | |
|---|---|---|---|---|---|---|---|
| Ballast Type | Trial 1 | Trial 2 | Trial 3 | Trial 4 | Trial 5 | Average (lbs) | Friction coefficient |
| I | 121.2 | 119.55 | 113.85 | 112.75 | 116.75 | 116.82 | 0.23 |
| II | 74.1 | 71.6 | 78.25 | 74.65 | 71.7 | 74.06 | 0.25 |
| II | 67.3 | 63.95 | 58.55 | 59.95 | 59.2 | 61.79 | 0.34 |

# CHAPTER SEVEN

# CONCLUSION AND FUTURE WORK

The main aim of this project was to provide International Fabrics Association Industrial (IFAI) with the minimum ballast weight values that can safely hold various tents to the ground for the wind loads prescribed by code. Using Finite Element Analysis, Matlab scripts were created to model tents and return ballast weight values for a tent with a given configuration, type of ballast and surface region on which the tent was placed.

A Full Factorial Design of Experiments approach was used. The effect of the guy's pre-tension, wind speed for a region, tent's length, width and roof pitch angle on the ballast weight values were observed. It was found from this experiments that the higher the values of wind speed, guys' pre-tension, length, width, and roof pitch angle, the heavier the ballast weights. All the experiments in Matlab were carried out only in partially enclosed condition using Main Wind Force Resisting System (MWFRS) method.

This project has given way for future work to take other factors into account for determining and optimizing the values of ballast weights. The limitations of the method should be resolved. In particular, the ability to include the ability of the footings to lift should be included in conjunction with the application of pre-tension in guy lines. Additional research subjects should include studying the effect of frame stiffness and guy stiffness on ballast weight values, as well as the effect of enclosed and open conditions of walls on ballast weight values and finally, all the effects should be studied for Components and Cladding (C&C) method instead of MWFRS method.

## REFERENCES

[1] “Ballast”, Ballast, 14 Mar. 2016.

https://en.wikipedia.org/wiki/Ballast

[2] "Company Overview", Industrial Fabrics Association International, 14 Mar. 2016. www.ifai.com/about/

[3] Mohammadi, Jamshid, and Amir Zamani Heydari. “Seismic and Wind Load considerations for Temporary Structures.” Practice Periodical on Structural Design and Construction, vol. 13, no. 3, 2008, pp. 128–134.

[4] Bolduc, William T. “When the Roof Collapses.” Structures Congress 2011, 2011, pp. 1827-1838.

[5] Gorlin, William B. “Wind Loads for Temporary Structures: Making the Case for Industrywide Standards.” Journal of Architectural Engineering, vol. 15, no. 2, 2009, pp. 35–36.

[6] McAlpine, George. “Caution! FEA in Use.” Pipelines 2013, Nov. 2013, pp. 556 - 565.

[7] Mu, Bin, et al. “FEA of Complex Bridge System with FRP Composite Deck.” Journal of Composites for Construction, vol. 10, no. 1, 2006, pp. 79–86.

[8] Bail, Justin L. “Non-Destructive Investigation & FEA Correlation on an Aircraft Sandwich Composite Structure.” Earth and Space Conference 2008: Proceedings of the 11th Aerospace Division International Conference on Engineering, Science, Construction, and Operations in Challenging Environments, vol. 323, Apr. 2008.

[9] Lu, S. C., et al. “Integration of CAD and FEA for Concurrent Engineering Design of Sheet Stamping.” Journal of Manufacturing Science and Engineering, vol. 118, no. 3, 1996, pp. 310–317.

[10] Dinh, T.D., et al. “A Study of Tension Fabric Membrane Structures under in-Plane Loading: Nonlinear Finite Element Analysis and Validation.” Composite Structures, vol. 128, 2015, pp. 10–20.

[11] Zhao, Jiaxin. “Computer Application in Solving Statically Determinate Truss Problems Using FEA and Matlab.” Computer Applications in Engineering Education, vol. 17, no. 4, 2009, pp. 363–371.

[12] Pike, M. “Introducing Finite Element Analysis in Statics,” Proceedings of the 2001 American Society for Engineering Education Annual Conference & Exposition, 2001.

[13] St.Pierre, L.M., et al. Wind Loads on Houses: A Wind Tunnel Study. Institute for Catastrophic Loss Reduction Research Paper Series, 2003.

[14] Stathopoulos, Theodore, et al. “Wind Shielding Effects of Trees on Low Buildings.” Building and Environment, vol. 29, no. 2, 1994, pp. 141–150.

[15] Wang, Ronghui, et al. “Model Test and Numerical Analysis of a Special Joint for a Truss Bridge.” Journal of Constructional Steel Research, vol. 65, no. 6, 2009, pp. 1261–1268.

[16] Kurowski, P. "Good solid modeling, bad FEA." Machine Design International, vol. 68, no. 21, Nov. 1996, pp. 67–72.

[17] He, Lin, et al. “Parametric Modeling and Stability Analysis of Temporary Grandstand.” Applied Mechanics and Materials, vol. 578-579, 2014, pp. 907–916.

[18] American Society of Civil Engineers. *Minimum Design Loads for Buildings and Other Structures, Standard ASCE/SEI 7-10*. 2013.

[19] Hinton, E., and D. R. J. Owen. An Introduction to Finite-Element Computations. Pineridge Pr., 1985.

[20] "Design of Experiments – A Primer", iSixSigma, 6 Feb. 2016. https://www.isixsigma.com/tools-templates/design-of-experiments-doe/design-experiments-%E2%90%93-primer/

[21] "Overview", Matlab, 6 Feb. 2016. https://www.mathworks.com/products/matlab.html?s_tid=hp_products_matlab

[22] "Abaqus Unified FEA", Abaqus, 6 Feb. 2016. https://www.3ds.com/products-services/simulia/products/abaqus/abaquscae/

[23] "About ASCE", ASCE, 6 Feb. 2016. https://www.asce.org/about_asce/

[24] Summers J., Blouin V., *IFAI 2011: Testing and Performance Analysis of Tent Ballast*, Report submitted to Industrial Fabrics Association International, Clemson University, April 2012.